BIOCHEMISTRY
including biophysical chemistry & molecular biology
Article

Biochemistry **2009,** *48,* 12113–12124 12113
DOI: 10.1021/bi901187u

Communication between R481 and Cu_B in Cytochrome bo_3 Ubiquinol Oxidase from *Escherichia coli*†

Tsuyoshi Egawa,‡ Myat T. Lin,§ Jonathan P. Hosler,∥ Robert B. Gennis,§ Syun-Ru Yeh,*,‡ and Denis L. Rousseau*,‡

‡*Department of Physiology and Biophysics, Albert Einstein College of Medicine, Bronx, New York 10461,* §*Department of Biochemistry and Chemistry, University of Illinois at Urbana−Champaign, Urbana, Illinois 61801, and* ∥ *Department of Biochemistry, University of Mississippi Medical Center, Jackson, Mississippi 39216*

Received July 11, 2009; Revised Manuscript Received October 29, 2009

ABSTRACT: The R481 residue of cytochrome bo_3 ubiquinol oxidase from *E. coli* is highly conserved in the heme−copper oxidase superfamily. It has been postulated to serve as part of a proton loading site that regulates proton translocation across the protein matrix of the enzyme. Along these lines, proton pumping efficiency has been demonstrated to be abolished in many R481 mutants. However, R481Q in bo_3 from *E. coli* has been shown to be fully functional, implying that the positive charge of the arginine is not required for proton translocation [Puustinen, A. and Wikström, M. (1999) Proc. Natl. Acad. Sci. U.S.A. *96*, 35−37]. In an effort to delineate the structural role of R481 in the bo_3 oxidase, we used resonance Raman spectroscopy to compare the nonfunctional R481L mutant and the functional R481Q mutant, to the wild type protein. Resonance Raman data of the oxidized and reduced forms of the R481L mutant indicate that the mutation introduces changes to the heme o_3 coordination state, reflecting a change in position and/or coordination of the Cu_B located on the distal side of heme o_3, although it is ∼10 Å away from R481. In the reduced-CO adduct of R481L, the frequencies of the Fe−CO and C−O stretching modes indicate that, unlike the wild type protein, the Cu_B is no longer close to the heme-bound CO. In contrast, resonance Raman data obtained from the various oxidation and ligation states of the R481Q mutant are similar to those of the wild type protein, except that the mutation causes an enhancement of the relative intensity of the β conformer of the CO-adduct, indicating a shift in the equilibrium between the α and β conformers. The current findings, together with crystallographic structural data of heme−copper oxidases, indicate that R481 plays a keystone role in stabilizing the functional structure of the Cu_B site through a hydrogen bonding network involving ordered water molecules. The implications of these data on the proton translocation mechanism are considered.

Heme−copper oxidases are the terminal enzymes of the electron transport chains in the inner mitochondrial membrane of eukaryotes and in the cytoplasmic membrane of bacteria (*1*). The enzymes catalyze the four-electron reduction of dioxygen to water at a catalytic site formed by a binuclear center, consisting of a high-spin heme (heme a_3 of cytochromes aa_3 and ba_3 or heme o_3 of cytochrome bo_3[1]) and a copper atom (Cu_B). In addition to the heme−copper binuclear center, the enzymes have a low-spin heme group (heme *a* of cytochromes aa_3 or heme *b* of cytochromes ba_3 and bo_3), which mediates electron transfer to the binuclear center (*1*).

In heme−copper oxidases, four protons are taken up from the negative side (n-side) of the mitochondrial/cytoplasmic membrane, which are consumed for the reduction of a dioxygen molecule to water. During the oxygen reaction, four additional protons are pumped across the membrane from the n-side to the positive side (p-side) of the mitochondrial intermembrane space or the periplasmic space (*1*). Proton conducting pathways in oxidases were first identified in bacterial enzymes by site-directed mutagenesis studies more than two decades ago (*2*, *3*). Later, X-ray crystallographic studies of the bacterial as well as mammalian oxidases have further clarified the structure of the proton conducting pathways. So far three pathways, H-, D-, or K-channels (named after one of the conserved amino acid residues in each postulated pathway) have been identified (*4*−*6*). The functional importance of the three channels in proton translocation, as well as in providing chemical protons for the dioxygen reduction reaction to water, has been extensively investigated (*2*, *3*, *7*−*15*); the data suggest that the D- and K-channels are essential for the function of the bacterial heme−copper oxidases (*2*, *3*, *7*−*9*, *11*−*13*), while the H-channel is functionally unique to mammalian oxidases (*10*).

It is well accepted that the D- and K-channels (Figure 1a) provide proton conducting pathways from the n-side surface of the protein to a proton loading site in the vicinity of the heme−copper center, ∼13 Å away from the p-side surface. It is, however, unclear as to how the protons are expelled from the proton loading site to the p-side. The propionate side chain groups of the two hemes, pointing toward the p-side of the membrane (Figure 1a) have been postulated to be part of the proton loading site (*16*−*22*). FTIR studies showed that the propionate groups of cytochrome *c* oxidase from *Paracoccus*

†This work was supported by the National Institutes of Health Grants GM56824 to J.P.H. and GM074982 to D.L.R; and Department of Energy Grant DE-FG02-87ER13716 to R.B.G.

*To whom correspondence should be addressed. (S.-R.Y.) Tel: 718-430-4234. Fax: 718-430-4230. E-mail: syeh@aecom.yu.edu. (D.L.R.) Tel: 718-430-3592. Fax: 718-430-8808. E-mail: rousseau@aecom.yu.edu.

[1]Abbreviations: cytochrome bo_3, cytochrome bo_3 quinol oxidase from *E. coli*; C*c*O, cytochrome *c* oxidase; bC*c*O, cytochrome *c* oxidase from bovine; RsC*c*O, cytochrome *c* oxidase from *Rhodobacter sphaeroides*; PdC*c*O, cytochrome *c* oxidase from *Paracoccus denitrificans*; RR, resonance Raman; ICP-OES, inductively coupled plasma optical emission spectroscopy; FTIR, Fourier transform infrared spectroscopy.

Published on Web 11/20/2009

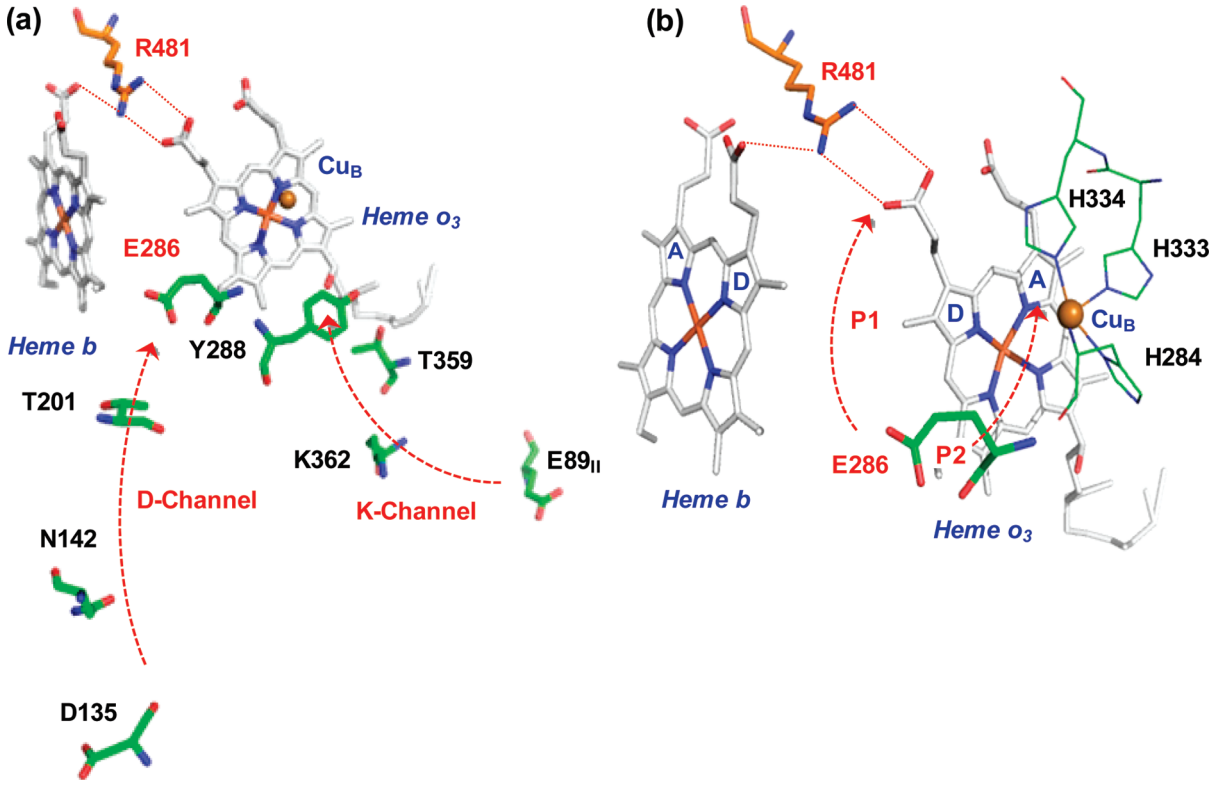

FIGURE 1: X-ray crystallographic structure of cytochrome bo_3. (a) The proton conducting D- and K-channels and the relative locations of the R481 and E286 residues with respect to hemes *b*, heme o_3, and Cu_B are illustrated. (b) The two putative proton exit pathways, which shuttle protons from E286 to the p-side of the membrane are shown; the P1 pathway represents a direct proton exit pathway from E286 to the H-bonded R481-heme propionate region, whereas the P2 pathway represents an alternative pathway via the Cu_B ligands. The hemes, Cu_B, and all of the amino acids shown here reside in subunit I, except for E89, which is from subunit II. The structure was rendered from PDB ID 1FFT with PyMOL (DeLano Scientific, LLC).

denitrificans (PdC*c*O) undergo conformational changes in response to the redox state changes of the two hemes, consistent with the possible functions of the propionate groups as proton traps during the catalytic cycle of the enzyme (*16*, *17*).

In the heme−copper oxidases, an arginine (R481 in the bo_3 numbering) located within hydrogen bonding distances to the D-propionates of the two hemes (Figure 1b) is highly conserved. The presence of such a positively charged amino acid is expected to stabilize the anionic form of the carboxyl groups and thereby regulate the protonation state of the propionates, forming an essential element of the proton loading site. However, the proposed role of the conserved R481 residue is not fully sustained by site-directed mutagenesis studies. Puustinen and Wikstrom observed that the mutation of R481 to glutamine in cytochrome bo_3 did not cause a significant loss of the pumping activity, although the mutation of R481 to nonpolar amino acids, such as methionine and leucine, or to neutral/polar asparagine, did abolish the proton pumping activity of the enzyme (*21*). More recently, Lee et al. (*23*) found 40% pumping efficiency in the R481L mutant of the *Rhodobacter sphaeroides* aa_3 oxidase (RsC*c*O), implying that the positive charge of R481 is not essential for the proton pumping function of the heme−copper oxidases, but resonance Raman (RR) data suggest that R481 is critical for the enzymatic function by stabilizing or maintaining the active site structures in a functional state (*24*). To examine the role of R481 in cytochrome bo_3, in this work we have systematically investigate the structural properties of R481Q and R481L mutants in various oxidation and coordination states by using RR and electronic absorption spectroscopy.

MATERIALS AND METHODS

Sample Preparation. The wild type and R481 mutants of *E. coli* bo_3 quinol oxidase were expressed and purified as described elsewhere (*25*). The proteins were dissolved in 50 mM potassium phosphate (pH 8.2) with 0.1% dodecyl maltoside. The fully reduced ligand-free form was prepared by reducing the samples with sodium dithionite under an argon atmosphere, while the reduced-CO form was obtained by introducing CO to the fully reduced samples. All chemicals were purchased from Sigma and used without further purification.

Metal Analysis. Metal content was measured by inductively coupled plasma optical emission spectroscopy (ICP-OES) using a Spectro Genesis spectrometer, as previously described (*26*). Before analysis, in order to eliminate adventitious divalent metals, the wild-type and R481L cytochrome bo_3 samples were dialyzed overnight into 10 mM Tris-HCl, 20 mM KCl, 1 mM EDTA, and 0.05% dodecyl maltoside at pH 8. The method yields the concentrations of Fe, Cu, Mg, Mn, Ca, Zn, Mo, and Ni as well as sulfur and phosphorus. Assuming the protein is pure, the concentration of the protein can be determined by the sulfur content as the sum of methionine and cysteine residues. For cytochrome bo_3, this comes to 80 mol of S per mol of enzyme.

Heme Analysis. Hemes were extracted from cytochrome bo_3 samples and analyzed by HPLC as previously reported (*27*). Five hundred microliters of fresh cold acidic acetone (acetone/HCl/H_2O; 9:1:1) was added to a sample containing 10 nmol of enzyme. The mixture was vortexed vigorously and centrifuged at 16000*g* for 2 min at 4 °C. The hemes in the supernatant were extracted with 600 μL of diethylether, washed with 600 μL H_2O, and dried

under a nitrogen stream. The dried heme extract was dissolved in 20 μL of an ethanol/acetic acid/H_2O mixture (70:17:13) and loaded onto a Miscrosorb-MV 100-5 C18 reverse-phase HPLC column (Varian, Palo Alto, CA) fitted to a Waters 600 HPLC pump with a mobile phase of the ethanol/acetic acid/H_2O mixture (70:17:13). The heme peaks were monitored at 402 nm by a Waters 2487 dual wavelength absorbance detector. At a flow-rate of 0.5 mL/min, heme B and heme O have retention times of about 4 and 8 min, respectively.

Quinone Analysis. Ubiquinone from cytochrome bo_3 was extracted and analyzed by HPLC as reported before (*27*). Ten nanomoles of cytochrome bo_3 and 10 nmol of ubiquinone-10 (Q-10) were mixed and diluted to 1 mL with water. Q-10 was added as an internal standard. Three milliliters of a methanol/petroleum ether (3:2) solvent was added to the mixture, which was then vortexed vigorously and centrifuged briefly. The upper organic layer containing the ubiquinones was transferred to a fresh tube, and the remaining mixture was extracted with 1.5 mL of petroleum ether two more times. All of the extracts were combined and dried under a nitrogen stream. The ubiquinone extracts were dissolved in 20 μL of ethanol and analyzed with the same HPLC equipment used in the heme analysis with a mobile phase of ethanol/methanol/acetonitrile (4:3:3). At a flow rate of 0.8 mL/min, the 278 nm peaks for ubiquinone-8 (Q-8) and Q-10 have retention times of about 9 and 19 min, respectively. We found that each of the proteins contained ~1 Q-8 molecule per protein molecule.

Raman and Optical Measurements. The resonance Raman spectra were carried out as previously described (*28*). Briefly, the 413.1 nm excitation from a Kr ion laser (Spectra-Physics, Mountain View, CA) was focused to an ~30 μm spot on the spinning quartz cell rotating at ~1,000 rpm. The scattered light, collected at a right angle to the incident laser beam, was focused on the 100 μm-wide entrance slit of a 1.25 m Spex spectrometer equipped with a 1200 grooves/mm grating (Bausch & Lomb, Analytical Systems Division, Rochester, NY), where it was dispersed and then detected by a liquid nitrogen-cooled CCD detector (Princeton Instruments, Trenton, NJ). A holographic notch filter (Kaiser Optical Systems, Ann Arbor, MI) was used to remove the laser line. The Raman shift was calibrated with indene. Unless otherwise stated, the laser power was kept < 4 mW for all measurements to avoid photodamage to the protein. Optical absorption spectra were measured on a Shimadzu UV2100U spectrophotometer.

RESULTS

To explore the structural and functional roles of the R481 residue in cytochrome bo_3 quinol oxidase from *E. coli*, we have replaced the positively charged arginine with a neutral amino acid, leucine or glutamine. It has been shown that the proton pumping activity in R481L was abolished, while that in R481Q was retained (*21*), although the steady state activity is partially preserved in both mutants (*vide infra*). The present preparations of the mutant proteins confirmed the reported functional properties, the details of which will be reported elsewhere (Lin et al., manuscript in preparation).

Analyses of the Metal and Heme Content of Cytochrome bo_3. To examine if the abolishment of the proton pumping activity in R481L is a result of the loss of heme O and/or Cu_B in the binuclear center, we performed metal and heme content analysis. As listed in Table 1, the wild type enzyme has the expected copper content (1 copper per enzyme molecule) but is slightly deficient (1.7 vs 2.0) in Fe, perhaps due to some loss of heme during sample preparation. The R481L mutant, however, shows that there is a substantial loss of both Fe and Cu. This coincides with a deficiency of heme O compared to heme B. Altogether, the data indicate that the R481L mutation results in severe disruption of the heme o_3-Cu_B active site, corresponding to the loss of the metals in the heme o_3-Cu_B site in about 40% of the enzyme population. The observed steady state activity of the R481L mutant is hence attributed to the fraction of the protein population that retains the active-site metals.

Table 1: Metal and Heme Contents of wt and R481L Mutant of Cytochrome bo_3 Proteins

	Cu[a]	Fe[a]	Heme B/Heme O
wt	0.96	1.7	1:0.88
R481L	0.53	1.3	1:0.54

[a]The Cu and Fe amounts reported were per cytochrome bo_3 complex as estimated from the amount of sulfur measured for the same samples by ICP-OES.

Electronic Absorption Spectra. Figure 2 shows the absorption spectra of the R481L (b) and R481Q (c) mutants, as compared to the wild type (wt) bo_3 enzyme (a), in the as-isolated (oxidized) state (thin solid lines), reduced state (dotted lines), and reduced CO-bound state (dot-dashed lines). The absorption peak positions are summarized in Table S1 in the Supporting Information. Although the positions of the absorption maxima of the mutant proteins are similar to those of the wt in each of the three states, the relative band intensities are significantly different. For example, R481L has a more intense Soret maximum and weaker α band in the CO-bound state, as compared to the wt protein, while R481Q has a more intense Soret maximum in the reduced state. The data indicate that the mutations perturb the electronic structure of hemes *b* and/or o_3, although some of these differences could result from the slight differences in the metal and heme contents. To differentiate whether the spectral changes originated from heme *b* or o_3, we subtracted the reduced spectrum from the CO-bound spectrum. The contributions from heme *b* are expected to be the same in both spectra; therefore, they cancel out in the difference spectrum, resulting in an o_3^{2+}-CO *minus* o_3^{2+} spectrum. When we generated the CO difference spectra, the R481Q mutant showed a spectrum very close to that of the wt protein (bold lines in Figure 2, panels a and c, and Table S1, Supporting Information). This suggests that the changes in the intensities in the absorption spectra of the reduced and CO-bound forms of the R481Q mutant do not originate from the o_3 heme but rather from the b^{2+} heme. However, the difference spectrum of the R481L mutant is significantly different from that of the wt protein, indicating that the heme o_3 site is altered in this mutant.

Resonance Raman (RR) Spectra of the Oxidized Forms. In prior RR studies of the bo_3 oxidase, the oxidized enzyme was found to be photoreduced when exposed to a laser beam for the Raman measurements (*29*, *30*). To avoid photoreduction that may complicate spectral assignments, we first examined the laser power-dependence of the RR spectra of the oxidized forms. The two wt spectra shown in Figure 3a were obtained with laser powers of 1 mW (solid line) and 3 mW (dotted line). The intensity of the 3 mW spectrum was normalized so that the amplitude of the most intense RR band (ν_4 at 1375 cm^{-1}) was comparable to that of the 1 mW spectrum. As can be seen, at 1 mW, a small

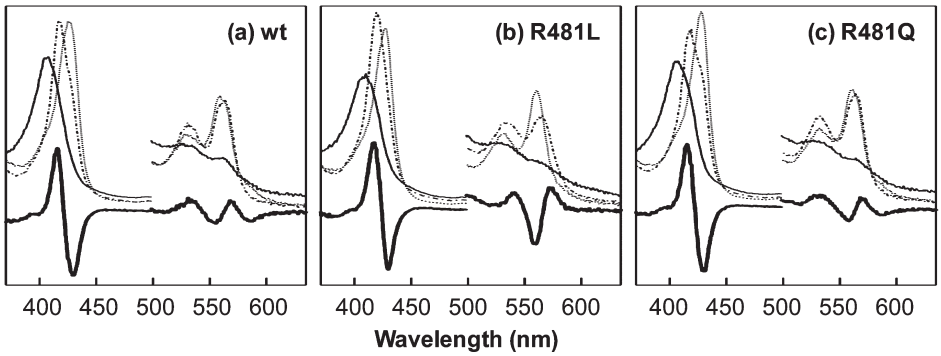

FIGURE 2: Electronic absorption spectra of the wt (a) and R481L (b) and R481Q (c) mutants of cytochrome bo_3 in the oxidized (thin solid line), reduced ligand-free (dotted line), and reduced CO-bound (dot-dashed line) states. The bold solid line at the bottom of each panel shows the CO-bound minus reduced ligand-free difference spectrum.

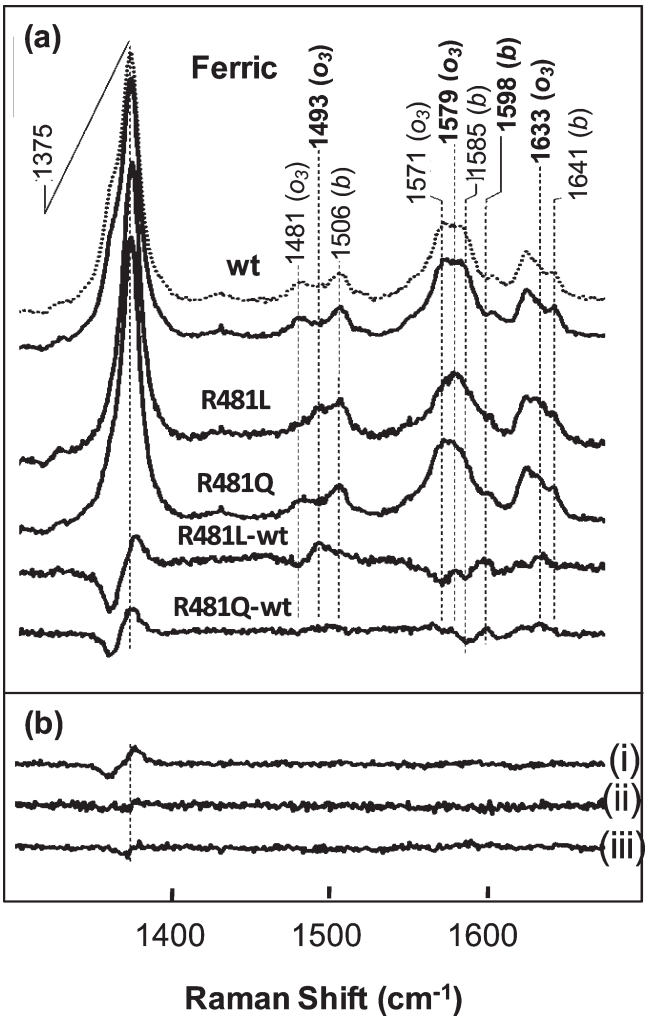

FIGURE 3: Resonance Raman spectra of the oxidized forms of the wt and the R481L and R481Q mutants of cytochrome bo_3 (a) and their associated laser power difference (1 mW minus 3 mW) spectra (b). The R481L-wt and R481Q-wt difference spectra are shown at the bottom in (a). The frequencies of the new modes in the mutants are highlighted in bold. The wt spectra shown in (a) are those obtained with the laser power of 1 mW (solid line) or 3 mW (dotted line). The power difference spectra for wt, R481L, and R481Q are shown as the top (i), middle (ii), and bottom (iii) traces, respectively, in (b). The excitation wavelength for the Raman measurements was 413.1 nm, and the laser power was 1 mW unless indicated otherwise.

shoulder on the low frequency side of the ν_4 mode was present, indicating a small amount of photoreduction. This shoulder is slightly more pronounced at 3 mW. As highlighted in the 1 mW *minus* 3 mW difference spectrum [Figure 3b, difference spectrum i], a derivative-like feature in the 1375 cm^{-1} region was observed, confirming the additional photoreduction at the higher power. Similar power-dependence experiments were performed with the R481L and R481Q mutants. Interestingly, the mutant proteins did not show detectable photoreduction (difference spectra ii and iii in Figure 3b), giving additional evidence that the electronic structures of the heme(s) are somewhat altered in the mutants. On the basis of the power-dependence experiments, we compared the RR spectra of the wt protein and mutants obtained with the minimum laser power (1 mW).

The high frequency RR spectra of oxidases are in general dominated by the spin and coordination state marker lines of the two hemes (*31*, *32*). In the wt spectrum (Figure 3a and Table 2), the bands at 1585, 1506, and 1641 cm^{-1} are assigned to the ν_2, ν_3, and ν_{10} modes, respectively, of the 6-coordinate low spin (6C-LS) heme *b*; while those at 1571 and 1481 cm^{-1} are assigned to the ν_2 and ν_3 modes of the 6-coordinate high spin (6C-HS) heme o_3. In the R481L mutant, new bands appeared near 1493 and 1633 cm^{-1} at the expense of the ν_3 (1481 cm^{-1}) and ν_{10} (1641 cm^{-1}) band intensities of heme o_3 in the wt protein (see the R481L spectrum and the R481L-wt difference spectrum shown at the bottom). Such results are consistent with changes at heme o_3 upon mutation.

The frequencies of the new ν_3 and ν_{10} bands are indicative of the presence of a 5-coordinate high spin (5C-HS) heme o_3 (*31*, *32*). However, the RR intensities of the ν_3 (1506 cm^{-1}) and ν_{10} (1641 cm^{-1}) modes of heme *b* were unchanged, although the ν_2 RR band at 1585 cm^{-1} is weaker in the mutant and may have broadened and/or shifted to lower frequency. In addition, the intensity of ν_{37} at 1598 cm^{-1} from heme *b* has increased in intensity. Both ν_2 and ν_{37} are C_β−C_β stretching modes of the porphyrin core (*31*, *32*). We noted that the ν_2 mode may also broaden and/or shift to lower frequency upon mutation. Taken together, the RR data show that the distal water ligand coordinated to the heme o_3 in the wt protein (*33*, *34*) is absent in R481L as indicated by its 5C-HS configuration; in addition, the data indicate that heme *b*, like that in the wt protein, has a 6C-LS configuration, although the electronic structure of the mutant is slightly different from that of the wt protein. In contrast to R481L, changes were not detected in the heme o_3 marker bands of R481Q, although a small change in ν_2 of heme *b*, similar to that found in R481L, was observed. These observations are consistent with the results of the electronic absorption measurements, which indicated that there were changes in heme *b* of R481Q but not in heme o_3.

Table 2: Frequencies of the RR Bands and Coordination/Spin States of the Hemes *b* and o_3 of Cytochrome bo_3 Proteins[a]

	ν_2	ν_3	ν_4	ν_{10}	ν_{Fe-CO}	$\nu_{C=O}$	coordination- spin states*
oxidized							
wt							
$b + o_3$			1375				
b	1585	1506	-	1641			6C-LS
o_3	1571	1481	-	--			6C-HS
R481L							
$b + o_3$			1375				
b	-	1506	-	1641			6C-LS
o_3	1579	1493	-	1633			5C-HS
R481Q							
$b + o_3$			1375				
b	-	1506	-	1641			6C-LS
o_3	1571	1481	-	--			6C-HS
reduced forms							
wt							
$b + o_3$			1360				
b	1587	1491	-	--			6C-LS
o_3	1575	1473	1354[b]	1611			5C-HS
R481L							
$b + o_3$			1361				
b							
o_3	1583[c]	1471/1495[d]	1379[b],[e]	--			5C-HS/6C-LS
R481Q							
$b + o_3$			1360				
b	--	1491	-	--			6C-LS
o_3	1575	1473	1355[b]	--			5C-HS
CO-bound[f] forms							
wt − o_3	1592	1499	1369	1636	521	1960	6C-LS
R481L − o_3	1590	1501	1373	1634	521/495	1964[g]	6C-LS
R481Q − o_3	1590	1499	1370	1636	521/495[h]	1960/1947	6C-LS

[a] "-" stands for not determined, due to overlap of RR signals from hemes *b* and o_3 o; "--" stands for not clearly observed; * 5C and 6C stand for 5-coordinate and 6-coordinate, respectively; HS and LS stand for high spin and low spin, respectively. [b] Approximate frequencies obtained from the trough positions in the CO-reduced difference spectra. [c] RR band of the 6CLS component. [d] Approximate value of the 6CLS component determined on the basis of the difference spectrum with respect to the wt spectrum. [e] Attributed to both the 5CHS and 6CLS components. [f] Frequencies of porphyrin core modes obtained from the peak positions of the CO-reduced difference spectra. [g] Frequency of the major component. [h] Frequency of the shoulder.

In addition to the changes in the spin and coordination marker bands, small differences in the ν_4 mode at 1375 cm^{-1} in the mutants are evident in the difference spectrum. However, owing to a small amount of photoreduction in the wt protein (even at a power of 1 mW), a possible small shift in the mode from either of the hemes in both mutants would be obscured.

RR Spectra of the Reduced Forms. Figure 4 shows the RR spectra of the reduced forms of the R481L and R418Q mutants, as compared to the wt protein. The wt spectrum exhibits bands from 5C-HS heme o_3 at 1473 (ν_3), 1575 (ν_2), and 1611 (ν_{10}) cm^{-1}, and those from 6C-LS heme *b* at 1491 (ν_3) and 1587 (ν_2) cm^{-1}. The RR band at 1621 cm^{-1} is attributable to the vibrational modes of the vinyl side chains of both hemes (*35*), although ν_{10} of heme *b* might also contribute to the RR intensity at this frequency.

In the spectrum of R481L, the spectral intensity in the 1490−5 cm^{-1} region slightly increased at the expense of the ν_3 mode at 1473 cm^{-1} from heme o_3; in addition, a new band appeared at 1583 cm^{-1} with a concomitant weakening of the ν_2 mode at 1575 cm^{-1} from heme o_3 (see the R481L-wt difference spectrum). Furthermore, the ν_{10} band of heme o_3 at 1611 cm^{-1} weakened, although it is unclear if a new ν_{10} band emerged because the nearby 1621 cm^{-1} band also shifted slightly, which masked the possible spectral changes in the ν_{10} mode. These observations imply that heme o_3 in R481L is mainly in a native-like 5C-HS form, with a minor population of a 6C-LS form. The spectral changes found in R481L were not observed in R481Q, although there were small spectral changes in the 1620 cm^{-1} region.

We noted that the ν_4 band increased in frequency in both mutants. As in the oxidized enzyme, ν_4 from both hemes *b* and o_3 exhibits similar frequencies; thus, the origin of the shift cannot be determined unequivocally from these spectra alone. However, as the difference is significantly larger in the difference spectrum of the R481L mutant than that of the R481Q mutant, it is likely that the shift originates from the o_3 heme. Additional insights into the origin of the differences in the ν_4 region were obtained from a comparison with the CO spectra (*vide infra*).

RR Spectra of the CO Forms. Figure 5a shows the high frequency RR spectra of the CO derivatives of the R481L and R481Q mutants as compared to the wt protein. The laser power used for the RR measurements was kept low (1 mW) to avoid photodissociation of CO (the RR spectra shown here, as well as the low frequency spectra that cover the Fe-CO stretching bands, did not show photodissociation-dependent changes within 100 μW−1 mW laser power under our experimental conditions; see Figures S1 and S2 in the Supporting Information). In the CO-derivative, the ν_4 mode from heme *b* and heme o_3 is expected to be well separated, with the former in the 1360 cm^{-1} region (as found in the reduced spectrum) and the latter in the 1370−75 cm^{-1} region as found in the CO-adducts of other heme proteins (*28*). Surprisingly, large differences were found in the relative intensities of these two modes in the wt protein and the two mutants. In the wt protein, the ν_4 mode is broad and centered at 1363 cm^{-1}, indicating that the spectrum is dominated by heme *b*. A similar spectrum was observed for the R481Q mutant,

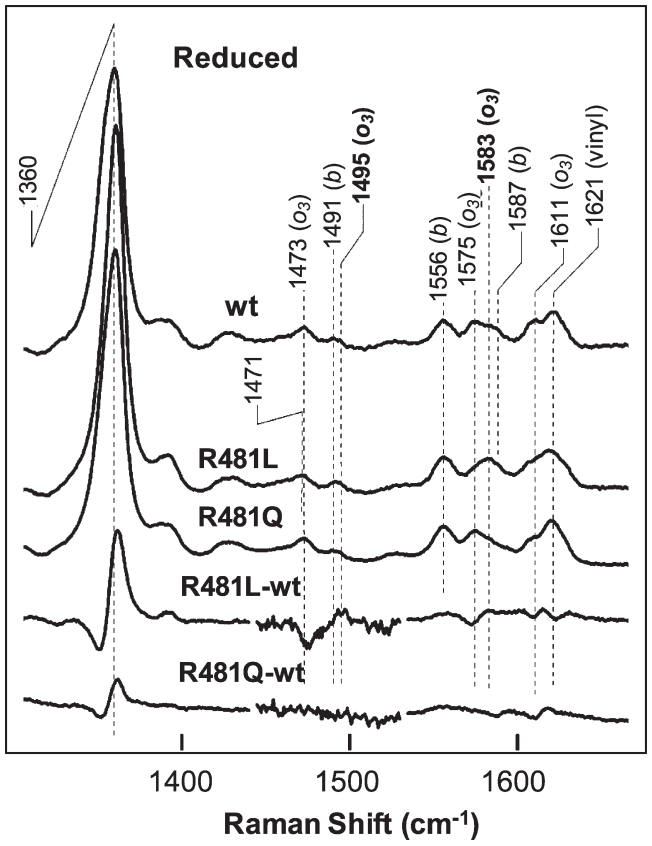

FIGURE 4: Resonance Raman spectra of the reduced forms of the wt and the R481L and R481Q mutants of cytochrome bo_3. The R481L-wt and R481Q-wt difference spectra are shown at the bottom. The 1445−1530 cm^{-1} region of the difference spectra were expanded vertically by a factor of 5 as compared to the other region of the spectra to magnify the spectral changes. The frequencies of the new modes in the mutants are highlighted in bold. The excitation wavelength for the Raman measurements was 413.1 nm.

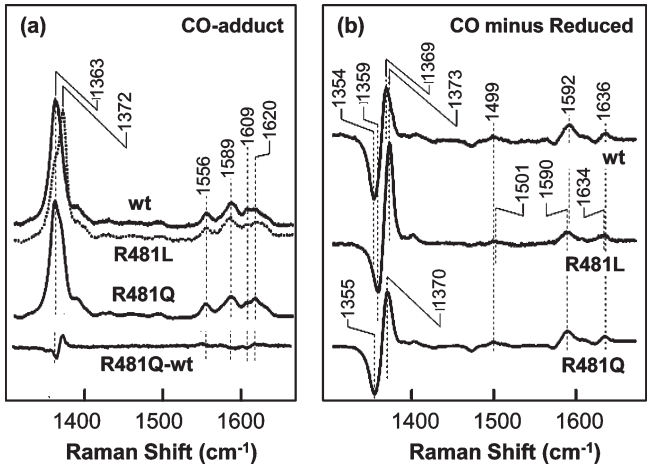

FIGURE 5: Resonance Raman spectra of the CO-bound forms of the wt and the R481L and R481Q mutants of cytochrome bo_3 (a) and their associated CO-bound minus reduced ligand-free difference spectra (b). To obtain the difference spectra shown in (b), the reduced spectrum of each protein taken from Figure 4 was subtracted from the corresponding spectrum shown in (a), and the two spectra were normalized with respect to the heme *b* mode at 1556 cm^{-1} such that it was canceled out in the resulting difference spectra. The frequencies of the new modes in the mutants are highlighted in bold. The excitation wavelength for the Raman measurements was 413.1 nm.

although a prominent shoulder appeared at a higher frequency. In contrast, in the R481L mutant, the ν_4 line was located at 1372 cm^{-1} with a shoulder at 1363 cm^{-1}, indicating that the spectrum is dominated by the CO-bound heme o_3. It is important to note that there is no evidence in the data for photooxidation that would give an oxidized heme *b*, yielding a spectrum with a strong ν_4 band in the 1372 cm^{-1} region, as observed in the R481L mutant; in addition, there is no evidence in the data for photodissociation of the CO from heme o_3, which would give a strong line in the 1360 cm^{-1} region, as observed in the wt protein and the R481Q mutant. Thus, we attribute the observed differences in the ν_4 region of the spectra to a difference in the electronic transitions, resulting in differences in the relative enhancements of heme *b* and heme o_3. However, we are cognizant that this difference in the R481L mutant could be affected by metal and heme loss.

To sort between the contributions from the two hemes, difference spectra of the CO-bound minus the ligand-free reduced form were calculated, as was done for the optical absorption spectra (Figure 2). Prior to subtraction, we normalized the intensity of two spectra with respect to the heme *b* mode at 1556 cm^{-1}, which was seen in the spectra of both the CO-bound and the ligand-free reduced forms, with the same center frequency and width. In the difference spectra, the spectral contributions from heme *b* are canceled out, and a pure CO-bound minus reduced heme o_3 difference spectrum is expected. Figure 5b shows the CO difference spectra of the wt protein and the R481L and R481Q mutants thus obtained. As in the difference spectra, the ν_4 modes of the CO-adduct and reduced form of the heme o_3 show up as a positive and negative peak, respectively, and we assigned the ν_4 mode of the reduced heme o_3 of the wt protein, the R481Q mutant, and R481L mutant at 1354, 1355, and 1359 cm^{-1}, respectively, and the corresponding frequencies of the CO-bound heme o_3 at 1369, 1370, and 1373 cm^{-1}. The data show significant changes in heme o_3 of R481L, but not R481Q, although those in the reduced heme of R481L may be a consequence of its conversion to a mixture of the 5C-HS and 6C-LS forms (see above). On the basis of the difference spectra, frequencies of the other marker bands of heme o_3, ν_{10} at1636 cm^{-1} and ν_2 at1592 cm^{-1}, were also estimated for the wt protein and were found to be unchanged in the mutants. The frequencies of the marker bands are summarized in Table 2, together with the assigned coordination and spin states of the hemes.

CO has been shown to be a useful probe for the investigation of the distal environment of heme proteins (*28*, *36*). To determine the Fe−CO stretching mode (ν_{Fe-CO}), C−O stretching mode (ν_{C-O}), and Fe−C−O bending (δ_{Fe-C-O}) mode, we performed $^{12}C^{16}O-^{13}C^{18}O$ isotope substitution experiments. As shown in Figure 6a, the isotope sensitive bands of the wt protein at 521 and 573 cm^{-1} are assigned as the ν_{Fe-CO} and the δ_{Fe-C-O} modes, respectively, on the basis of the isotope shifts shown in Figure 6b (*29*, *30*, *37*). Similar spectra were obtained from the R481Q mutant. In contrast, the R481L protein exhibits a new ν_{Fe-CO} mode at 495 cm^{-1} together with a weaker ν_{Fe-CO} mode at 521 cm^{-1}. The detection of two ν_{Fe-CO} modes in R481L indicates the presence of two distinct conformers of the Fe−C−O moiety. Close examination of the wt and R481Q spectra revealed that both proteins contain a minor conformer with ν_{Fe-CO} at ~495 cm^{-1}, as evidenced by the shoulder of the 521 cm^{-1} band in the raw data (Figure 6a) and a weak trough at 478 cm^{-1} in the isotope difference spectra (Figure 6b). The data also show that the contribution of the minor conformer in R481Q

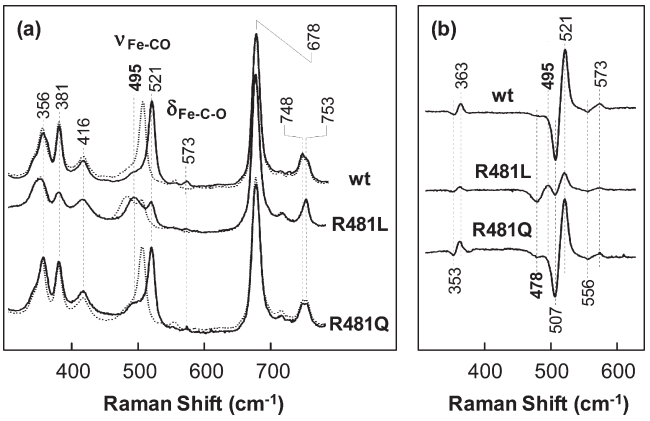

FIGURE 6: Low frequency resonance Raman spectra of the reduced CO-bound forms of the wt and the R481L and R481Q mutants of cytochrome bo_3 (a), and the associated $^{12}C^{16}O-^{13}C^{18}O$ isotope difference spectra (b). The RR spectra of the $^{12}C^{16}O$ and $^{13}C^{18}O$-adducts shown in (a) are presented in the solid and dotted lines, respectively. The frequencies of the new modes in the mutants are highlighted in bold. The excitation wavelength for the Raman measurements was 413.1 nm.

is slightly larger than that in the wt protein. The δ_{Fe-C-O} mode at 573 cm^{-1}, however, appeared to be unaffected by either mutation, although its intensity in the R481L mutant was significantly weaker than that in the wt.

In addition to the ν_{Fe-CO} and δ_{Fe-C-O} bands, the wt protein and mutants exhibit a weak isotope-dependent band at 363 cm^{-1} (Figure 6b), as reported for several other CO-bound heme proteins (*38*, *39*). Through a series of studies with deuterated heme, Rajani and Kincaid concluded that isotope sensitive bands in this region originate from vibrational coupling between ν_{Fe-CO} and heme deformation modes in this region (*39*). Although R481L exhibits two ν_{Fe-CO} modes, no additional isotope sensitive lines other than the 363 cm^{-1} band are observed, implying that the 363 cm^{-1} band arose through a vibrational coupling between the major ν_{Fe-CO} component at 521 cm^{-1} and a low-frequency mode of the porphyrin. Consistent with this hypothesis, the intensity of the 363 cm^{-1} band is much weaker in R481L than in the wt and the R481Q mutant.

The ν_{C-O} modes of the wt protein and the R481L and R481Q mutants were examined in the 1800−2050 cm^{-1} window. As shown in the $^{12}C^{16}O-^{13}C^{18}O$ isotope difference spectra (Figure 7), the ν_{C-O} mode of the wt protein was identified at 1960 cm^{-1}, in agreement with the reported IR data (*29*). It shifted to 1869 cm^{-1} with $^{13}C^{18}O$. The isotope shift of 91 cm^{-1} agrees well with the theoretical value predicted by assuming a C−O harmonic oscillator. The major ν_{C-O} modes at 1960 and 1869 cm^{-1} with $^{12}C^{16}O$ and $^{13}C^{18}O$ are accompanied by shoulders at 1947 and 1859 cm^{-1}, respectively. The shoulders are more prominent in R481Q, although the main peak positions at 1960 and 1869 cm^{-1} are unchanged. The R481L mutant has a significantly broader ν_{C-O} mode with the center position shifted to higher frequency by ~3−4 cm^{-1} as compared to the major ν_{C-O} modes of the wt protein and R481Q mutant. In addition, a weak but sharp contribution is present at 1960 cm^{-1}, the same frequency as the major ν_{C-O} modes of the wt protein and R481Q mutant. The significance of these data is discussed in the following section.

DISCUSSION

Substitution of the Arginine at position 481 with a leucine residue dramatically alters the structure and stability of the

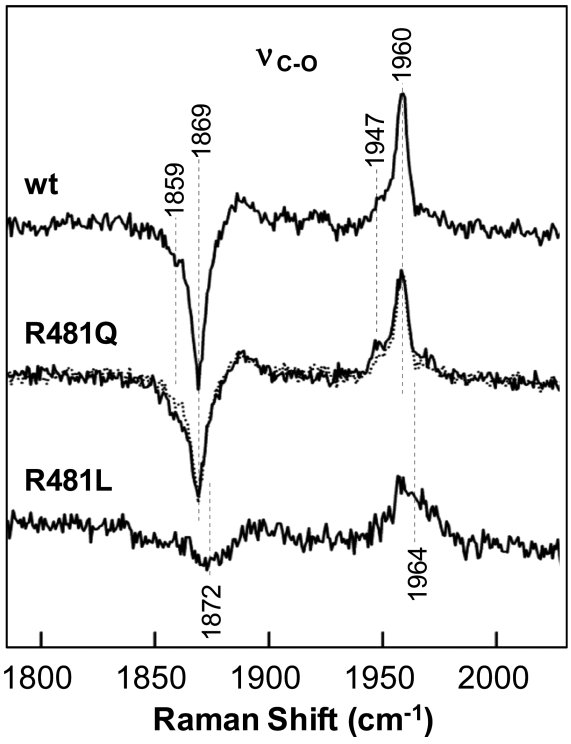

FIGURE 7: $^{12}C^{16}O-^{13}C^{18}O$ isotope difference spectra of the CO-adducts of the wt and the R481L and R481Q mutants of cytochrome bo_3. The R481Q spectrum is overlaid with the wt spectrum (dotted line) to highlight the band intensity changes.

Table 3: Comparison of the Properties of the R481 (R473 in PdC*c*O) Mutants of Various Oxidases[a]

protein	activity (%wt)	pumping	structure
	E. coli bo_3		
R481M	yes (2−8)[b]	no[b]	nd
R481L	yes (35−45)[b]	no[b]	modified[c]
R481N	yes (51−65)[b]	no[b]	nd
R481Q	yes (54−80)[b]	yes[b]	intact[c]
	RsC*c*O aa_3		
R481H	yes (18)[d]	yes[d]	modified[e]
R481K	yes (100)[f]	yes[f]	nd
R481L	yes (5)[d]	yes[d]	modified[e]
R481N	yes (6)[d]	no[d]	nd
R481Q	yes (4)[d]	no[d]	modified[e]
	PdC*c*O aa_3		
R473Q	no[g]	no[g]	modified[g]

[a]The activity is expressed as the percent of the wild type (wt), and the structure is based on the detection of changes in the resonance Raman spectra as defined in the text. [b]Ref *21*. [c]This work. [d]Ref *23*. [e]Ref *24*. [f]Refs *22* and *57*. [g]Ref *56*; nd, not determined.

binuclear center, as indicated by the loss of the heme o_3-Cu_B active site metals in about 40% of the population. To a first approximation, therefore, a maximum of 60% of the enzyme population must be responsible for the observed steady state activity (Table 3). The turnover number of the R481L mutant is ~35% to 40% of the wild type, normalized by the total heme content. Hence, the turnover per active enzyme molecule is likely to be somewhat higher than this value. Also, some of the differences in the spectroscopic properties of the mutant as

compared to the wt may have resulted from the reduced fraction of the heme o_3-Cu_B content in the R481L mutant.

Effects of Mutations on Heme b. Our recent study of cytochrome *c* oxidase from *Rhodobacter sphaeroides* has shown that mutations of residue R481 result in significant perturbations to both the low spin heme (heme *a*) and the heme a_3-Cu_B active site (*24*). In the current work, we have shown that the R481L mutant of cytochrome bo_3 does not substantially perturb low-spin heme *b*, although some modifications do occur. In the oxidized forms of R481L and R481Q of bo_3, the ν_3 mode of heme *b* at 1506 cm^{-1} was not perturbed, indicating that the heme remained 6C-LS. In contrast, the ν_2 and ν_{37} modes of heme *b*, which involve the C_β–C_β stretching mode of the porphyrin core (*31*, *32*), were slightly altered upon mutation. In the wt protein, R481 forms an H-bond with the propionate group attached to the D ring of heme *b* (see Figure 1b). Recent experimental and theoretical studies showed significant electronic conjugation between the propionate orbitals and porphyrin π-orbitals (*40*, *41*). Accordingly, we attribute the changes in the ν_2 and ν_{37} modes of heme *b* to the change in structural and electronic properties of C_β to which the propionate group is covalently linked. We hypothesize that the mutations alter the structure of the propionate which, in turn, change the planarity of the heme macrocycle and thus its vibrational spectrum. In addition, the proximal ligand of heme o_3 is H419, which is 2 residues in sequence away from H421, an axial ligand of heme *b*; the change in heme o_3 (*vide infra*) perhaps could affect the structural properties of heme *b* via the H419/H421 moiety. In summary, our data demonstrate that the mutations in R481 slightly affect the structural and electronic properties of heme *b*, although the origin of the spectral changes in heme *b* in the oxidized proteins remains to be further investigated.

Effects of Mutations on the Structure of Heme o_3. In contrast to the modest effects of the mutations on heme *b*, substituting R481 with a leucine residue dramatically alters the structure of the binuclear center. Our RR data, show that the distal environment of heme o_3 is perturbed significantly in this mutant, but it is not perturbed in R481Q. In particular, in the oxidized form of R481L, the sixth water ligand coordinated to heme o_3 found in the wt protein is absent; in addition, in the reduced form, the vacant sixth ligand binding site observed in the wild type protein is partially occupied by a non-native ligand. The latter finding suggests the coordination of an endogenous amino acid residue to the ferrous heme o_3 in R481L, as it is unlikely that a water molecule could be a sixth ligand of the ferrous heme. The distal pocket of heme o_3 is occupied by the Cu_B atom, which is coordinated by three histidine ligands (Figure 8). We hypothesize that the structure of the Cu_B site is perturbed in the R481L mutant, which destabilizes the coordination of the water ligand of heme o_3 in the oxidized state, and allows one of the histidine ligands of Cu_B (possibly H334; see Figure 8) to coordinate to heme o_3 in the reduced state, as no other endogenous ligands are accessible to the heme iron.

These large structural perturbations are somewhat surprising because the 481 position is quite remote from the Cu_B site (Figures 1 and 8). However, the reported crystallographic structures of heme–copper oxidases reveal the possible linkages between R481 and Cu_B. Although a set of full atomic coordinates including those of the ordered water molecules has not been reported for cytochrome bo_3, the positions of the ordered water molecules are available in crystal structures of cytochrome *c* oxidase from *Rhodobacter sphaeroides* (*42*), from *Paracoccus denitrificans* (*43*), and from bovine (*44*). Remarkably, in RsC*c*O (*42*), PdC*c*O (*43*), and bovine C*c*O (bC*c*O) (*44*), three water molecules were found to occupy virtually identical positions in the three distinct oxidases, on the basis of the crystallographic data. The three water molecules establish an H-bonding network linking R481 to the two heme propionate groups and one of the histidine ligands of Cu_B as shown in Figure 8. On the basis of the identity of the positions of these water molecules, we posit that related structured water molecules are present in the bo_3 structure as well and that they serve to stabilize the structure of the Cu_B center and its regioorientation with respect to the heme macrocycle. In the R481L mutant, the leucine cannot maintain H-bonding interactions; the structural integrity of the binuclear center is hence modified, resulting in the changes in the coordination state of heme o_3.

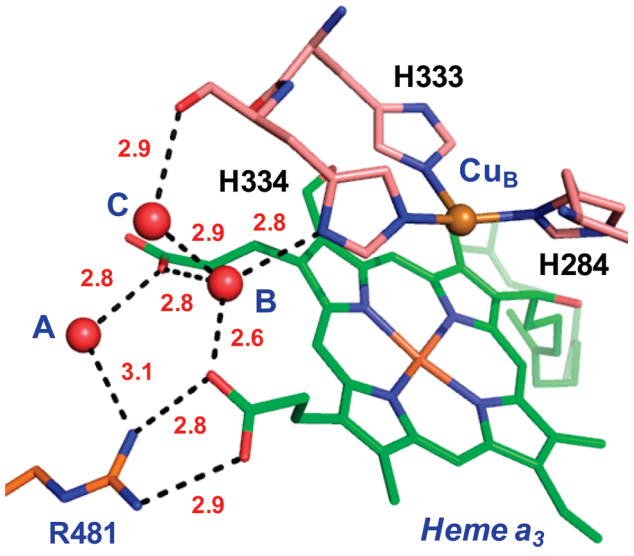

FIGURE 8: H-bonding network linking R481 to the Cu_B site in *R. sphaeroides* C*c*O. A, B, and C indicate the three water molecules mediating the H-bonding network involving R481, the D-propionate group of heme o_3, and H334 (one of the three Cu_B ligands). The H-bonding interactions (< 3.1 Å) are indicated by the dashed lines. The structure was rendered from PDB ID 2GSM with PyMOL (DeLano Scientific, LLC).

α and β Conformers of the CO-Bound Form. The binuclear center of the C*c*O family of proteins has been shown to exhibit two conformations in the presence of CO in the resonance Raman spectra (*45*, *46*). The discovery of 2 conformers of the CO-complex of C*c*O was first made by Alben and co-workers in low temperature photolysis studies of bovine mitochondria, rat heart myocytes, and opossum heart tissue slices with FTIR (*47*–*50*). Similar conformers of the CO-adduct of bacterial C*c*O were identified in RsC*c*O with FTIR by Gennis and co-workers (*51*–*53*). One conformer, termed the α form, has a higher ν_{C-O} frequency (1964 cm^{-1} for bC*c*O and 1966 cm^{-1} for RsC*c*O) as compared to that of the other conformer, termed the *β* form (1952 cm^{-1} for bC*c*O and 1955 cm^{-1} for RsC*c*O) (*45*, *46*). The ν_{Fe-CO} frequencies in these conformers were also determined for RsC*c*O at 519 (α form) and 493 (*β* form) cm^{-1}, although for bC*c*O only the α conformer with a ν_{Fe-CO} at 520 cm^{-1} was observed (*46*).

The ν_{Fe-CO} and ν_{C-O} frequencies of heme proteins are typically related by the well-established inverse correlation curve. For example, most of the data from histidine-ligated heme proteins, such as hemoglobins and myoglobins, fall on a linear

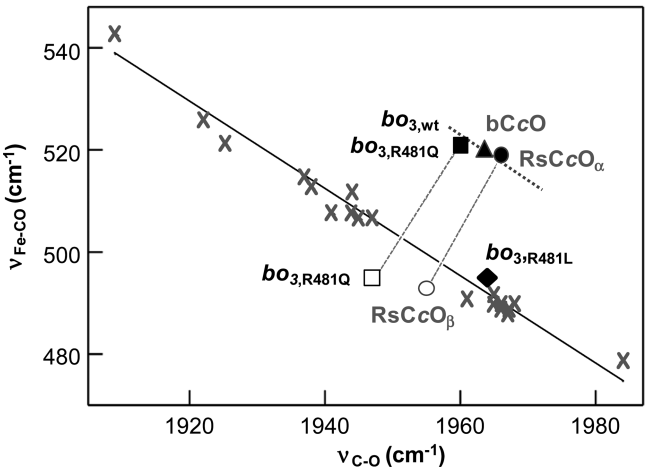

FIGURE 9: ν_{Fe-CO} versus ν_{C-O} inverse correlation plot of heme proteins. Data from hemoglobins, myoglobins and their distal mutant proteins are indicated by diagonal crosses. The solid line is the linear correlation obtained by a least-squares fit of the data. The data of heme−copper oxidases are indicated by a closed triangle (bovine C*c*O), a closed circle (α conformer of *R. sphaeroides* C*c*O), an open circle (*β* conformer of *R. sphaeroides* C*c*O), a closed square (the major component of wt and R481Q mutant of cytochrome bo_3), an open square (minor component of R481Q mutant of cytochrome bo_3), and a closed diamond (the major component of the R481L mutant of cytochrome bo_3). The data of hemoglobins and myoglobins are taken from ref *36* and references therein; bovine C*c*O and rsC*c*O are taken from ref *46*; wt and mutants of cytochrome bo_3 are from this work.

line (diagonal crosses in Figure 9). The offset of a correlation line is determined by the electronic properties of the proximal heme ligand. Consequently, the data associated with heme proteins with histidine as a proximal ligand stay on a line distinct from the P450 line with thiolate as a proximal ligand (not shown) and from the line associated with five coordinate CO-bound heme complexes. The positioning of a data point in a given correlation line, however, depends on the electrostatic environment of the heme-bound CO; when CO is exposed to a positive polar environment, the data point is located in the upper-left corner correlation; as the positive electrostatic environment of CO is reduced, the data points shift along the correlation line to the lower right corner. Although the C*c*O family of enzymes possesses a heme group with histidine as the proximal ligand, the data points associated with the α conformers of bC*c*O, RsC*c*O, and cytochrome bo_3 (with ν_{C-O} and ν_{Fe-CO} at 1960 and 521 cm^{-1}, respectively) do not lie on the inverse correlation line defined by the heme proteins with histidine as the proximal ligand (Figure 9) (*54*). The origin of this observation has been under intense debate. Nonetheless, it is generally agreed that the displacement of the C*c*O data from the histidine correlation line is a consequence of a strong interaction between Cu_B and heme-bound CO. Consistent with this conclusion, the reported crystal structure of the CO-bound C*c*Os shows that CO is highly bent because of its close proximity to Cu_B (*6*). In contrast to the behavior of the α-conformer, the *β* conformer lies close to the histidine correlation line (as demonstrated by the data associated with the *β* conformer of RsC*c*O shown in Figure 9), indicating a weaker interaction between CO and Cu_B.

Interestingly, like RsC*c*O, the R481Q mutant of cytochrome bo_3 possesses both α and *β* conformers. The data point for the major component, the α conformer with ν_{C-O} and ν_{Fe-CO} at 1960 and 521 cm^{-1}, like the wt protein, lies far above the histidine inverse correlation line in the plot (Figure 9, closed square), whereas the minor component has a data point (ν_{C-O}, 1947 cm^{-1}; ν_{Fe-CO}, 495 cm^{-1}) near the histidine correlation line (Figure 9, open square). Our RR data (Figure 6) indicate that, in the R481Q mutant, the equilibrium between the α and *β* conformers shifts slightly toward the former as compared to the wt protein, suggesting that the hydrogen bonding network linking R481 to the Cu_B site (Figure 8) regulates the α−*β* equilibrium.

However, the major component of R481L (with ν_{C-O} and ν_{Fe-CO} at 1965 and 495 cm^{-1}, respectively) lies on the histidine line, indicating that the strong influence of Cu_B exerted on CO is absent in this mutant. The position of the data point for the R481L mutant differs from that of the *β*-forms of the wt and the R481Q mutant. The frequency of the ν_{C-O} mode is more akin to that of the Y288F mutant of bo_3 in which it was concluded that the Cu_B was lost from the protein. This conformer was labeled the *δ*-form of the protein by Das et al. (*55*). This indicates that in R481L the hydrogen bonding network connecting R481 to the Cu_B site is disrupted such that there is no longer any interaction between Cu_B and bound CO. It is also noteworthy that the *β* conformer of R481Q, as well as the major component of R481L mutant, was found to be more resistant to the photodissociation than its α conformer (Figure S2 in the Supporting Information), although the origin of such a difference in photosensitivity is unclear.

Implications on the Proton Translocation Mechanism. In the catalytic cycle of heme−copper oxidases, the protons taken up from the n-side of the mitochondrial/cytoplasmic membrane are either consumed by dioxygen to form water molecules (chemical protons) at the binuclear center or pumped across the protein matrix to the p-side (pumped protons). The impact of mutations in the highly conserved R481 residues on the activity and proton pumping efficiency in various oxidases, including RsC*c*O, PdC*c*O, and bo_3 from *E. coli*, has been extensively studied. It was found that nearly all of the mutants retained some degree of activity, but only some mutants are competent to pump protons (see Table 3 and references therein).

The R481Q mutants are particularly interesting. In PdC*c*O, the mutation abolishes the activity and proton pumping capability; consistent with this, the RR data showed that the binuclear center was significantly modified (*56*). In RsC*c*O, the mutation leads to significant reduction of the activity (to 4% the native level) and total abolishment of the pumping efficiency (*23*); again the RR data are consistent with a modified binuclear center (*24*). In the bo_3 oxidase from *E. coli*, the mutation causes ~50% reduction in activity, while the proton pumping capability is retained (Lin et al., to be published) (*21*); as revealed in the present work, the mutation only resulted in small changes in the binuclear center. These data indicate that, depending on the protein, the R481Q mutation exerts differing effects on the stability of the binuclear center. Along these same lines, our present data show that the R481L mutant of bo_3 oxidase retains ~35−45% activity, but it does not pump protons, and its binuclear center is significantly perturbed. However, in the R481H and R481L mutants of RsC*c*O, proton pumping was observed, but the RR data showed that the catalytic site was significantly modified (*24*). In contrast, in the R481K mutant of RsC*c*O, both the activity and proton pumping capability are maintained, and the electronic absorption spectrum appears to be the same as that of the wt, indicating an intact binuclear center (although its RR data have not been obtained) (*22*, *57*). In summary, it is clear that mutations at this position may alter the structure of the heme sites and the catalytic activity, but whereas

catalytic activity is necessary for proton pumping, it is not sufficient in proteins with mutations at this position.

The mechanism by which the energy generated in the oxygen reduction process is coupled to proton translocation remains one of the major unsolved issues in the cytochrome oxidase field. Despite intense research, the identities of the proton pumping pathways remain controversial. Nonetheless, so far three proton pumping channels, D, K (Figure 1a), and H, have been suggested to pump the proton from the n-side of the mitochondrial/cytoplasmic membrane to a region near the binuclear center. However, albeit the fact that the D-channel has been clearly demonstrated in some bacterial oxidases, it is absent in the ba_3 oxidase from *Thermus thermophilus* (*58*); likewise, the H-channel has been implicated in mammalian C*c*O (*14*), but it is not functional in bacterial C*c*O (*10*). The proton loading sites, as well as the proton exit pathways, are also not well-defined. In any case, it will be quite remarkable if the differing oxidases with nearly identical catalytic sites use totally different mechanisms to couple the redox chemistry to the proton translocation.

It is well established that the D-channel in RsC*c*O, PdC*c*O, and bo_3 from *E. coli* delivers both chemical and pumped protons (*1*). The E286 residue at the end of the D-channel has been proposed to be a branching point, from which the protons are brought either to the binuclear center for the formation of water or toward a postulated proton exit channel (*1*). The D-propionate group of heme o_3 (a_3) is believed to be one of the proton loading site, accepting protons from E286 (*16*−*22*), although it is unclear how protons are transferred over such a long distance (see P1 pathway in Figure 1b), as there is no clear hydrogen bonding connection found between them in the crystal structures. Nonetheless, computer simulation studies have suggested that E286 and the D-propionate are connected via a number of as yet unresolved water molecules (*59*−*63*). In addition, an alternative route via the Cu_B site, indicated as the P2 pathway in Figure 1b, has been suggested (*64*−*66*).

The evidence presented in this study demonstrates that there is communication between R481 and the Cu_B site, possibly via a hydrogen bonding network involving the two propionates groups of heme o_3, three water molecules, and a Cu_B ligand, H334 (see Figure 8), supporting the P2 pathway. Presumably, the water molecules could facilitate proton movement along the P2 pathway (*67*). Consistent with this scenario, DFT and electrostatic calculations have implicated H334 as a critical proton pumping element (*68*). Additional water molecules identified recently in the crystal structure of rsC*c*O could facilitate proton movement along this pathway (*67*).

In order to ensure that the protons translocate against a gradient and to prevent slippage of the protons back to the n-side of the membrane, conformational changes are required. Recently, a large change in the position of heme a_3 was detected in the comparison between the oxidized and reduced forms of the aa_3 oxidase from *Rhodobacter sphaeroides* (*67*). This demonstrated a conformational flexibility of the heme that could be part of a regulatory mechanism for the control of proton translocation. Moreover, the data reported here show that the heme structure of the CO-bound adduct exists as an equilibrium between two conformers (α and β) of the protein and that this equilibrium, which was shown previously to exist in mitochondria and heart tissues (*47*, *49*, *50*) and which was shown to be pH dependent in rsC*c*O (*45*, *52*), is sensitively regulated by the 481 residue. While the presence of the two conformers has not been determined in the absence of CO, if the distinct conformers interchange during catalytic turnover, then it suggests that they may play a role in controlling the delivery of protons through the H-bonding network by regulating the linkage between the Cu_B ligands and the heme propionates with the associated H-bonded arginines. Further studies are needed to clarify the postulated proton affinity changes of the Cu_B cluster upon its $\alpha-\beta$ conversion and the role of other nearby residues. In summary, these results reported here support the structural role played by R481 in maintaining the functional H-bonding network that stabilizes the catalytic site of C*c*O and provide evidence for a potential pathway and control mechanism for the passage of pumped protons.

SUPPORTING INFORMATION AVAILABLE

Figures showing the power dependence of the resonance Raman spectra and a Table of the maxima in the optical spectra. This material is available free of charge via the Internet at http://pubs.acs.org.

REFERENCES

1. Branden, G., Gennis, R. B., and Brzezinski, P. (2006) Transmembrane proton translocation by cytochrome c oxidase. *Biochim. Biophys. Acta 1757*, 1052–1063.
2. Fetter, J. R., Qian, J., Shapleigh, J., Thomas, J. W., Garcia-Horsman, A., Schmidt, E., Hosler, J., Babcock, G. T., Gennis, R. B., and Ferguson-Miller, S. (1995) Possible proton relay pathways in cytochrome c oxidase. *Proc. Natl. Acad. Sci. U.S.A. 92*, 1604–1608.
3. Garcia-Horsman, J. A., Puustinen, A., Gennis, R. B., and Wikstrom, M. (1995) Proton transfer in cytochrome bo3 ubiquinol oxidase of *Escherichia coli*: second-site mutations in subunit I that restore proton pumping in the mutant Asp135→Asn. *Biochemistry 34*, 4428–4433.
4. Iwata, S., Ostermeier, C., Ludwig, B., and Michel, H. (1995) Structure at 2.8 A resolution of cytochrome c oxidase from *Paracoccus denitrificans*. *Nature 376*, 660–669.
5. Svensson-Ek, M., Abramson, J., Larsson, G., Tornroth, S., Brzezinski, P., and Iwata, S. (2002) The X-ray crystal structures of wild-type and EQ(I-286) mutant cytochrome c oxidases from *Rhodobacter sphaeroides*. *J. Mol. Biol. 321*, 329–339.
6. Yoshikawa, S., Shinzawa-Itoh, K., Nakashima, R., Yaono, R., Yamashita, E., Inoue, N., Yao, M., Fei, M. J., Libeu, C. P., Mizushima, T., Yamaguchi, H., Tomizaki, T., and Tsukihara, T. (1998) Redox-coupled crystal structural changes in bovine heart cytochrome c oxidase. *Science 280*, 1723–1729.
7. Belevich, I., Verkhovsky, M. I., and Wikstrom, M. (2006) Proton-coupled electron transfer drives the proton pump of cytochrome c oxidase. *Nature 440*, 829–832.
8. Brzezinski, P., and Adelroth, P. (1998) Pathways of proton transfer in cytochrome c oxidase. *J. Bioenerg. Biomembr. 30*, 99–107.
9. Konstantinov, A. A., Siletsky, S., Mitchell, D., Kaulen, A., and Gennis, R. B. (1997) The roles of the two proton input channels in cytochrome c oxidase from *Rhodobacter sphaeroides* probed by the effects of site-directed mutations on time-resolved electrogenic intraprotein proton transfer. *Proc. Natl. Acad. Sci. U.S.A. 94*, 9085–9090.
10. Lee, H. M., Das, T. K., Rousseau, D. L., Mills, D., Ferguson-Miller, S., and Gennis, R. B. (2000) Mutations in the putative H-channel in the cytochrome c oxidase from *Rhodobacter sphaeroides* show that this channel is not important for proton conduction but reveal modulation of the properties of heme a. *Biochemistry 39*, 2989–2996.
11. Pfitzner, U., Odenwald, A., Ostermann, T., Weingard, L., Ludwig, B., and Richter, O. M. (1998) Cytochrome c oxidase (heme aa3) from *Paracoccus denitrificans*: analysis of mutations in putative proton channels of subunit I. *J. Bioenerg. Biomembr. 30*, 89–97.
12. Ruitenberg, M., Kannt, A., Bamberg, E., Fendler, K., and Michel, H. (2002) Reduction of cytochrome c oxidase by a second electron leads to proton translocation. *Nature 417*, 99–102.
13. Ruitenberg, M., Kannt, A., Bamberg, E., Ludwig, B., Michel, H., and Fendler, K. (2000) Single-electron reduction of the oxidized state is coupled to proton uptake via the K pathway in *Paracoccus denitrificans* cytochrome c oxidase. *Proc. Natl. Acad. Sci. U.S.A. 97*, 4632–4636.
14. Shimokata, K., Katayama, Y., Murayama, H., Suematsu, M., Tsukihara, T., Muramoto, K., Aoyama, H., Yoshikawa, S., and Shimada, H. (2007)

The proton pumping pathway of bovine heart cytochrome c oxidase. *Proc. Natl. Acad. Sci. U.S.A. 104*, 4200–4205.
15. Tsukihara, T., Shimokata, K., Katayama, Y., Shimada, H., Muramoto, K., Aoyama, H., Mochizuki, M., Shinzawa-Itoh, K., Yamashita, E., Yao, M., Ishimura, Y., and Yoshikawa, S. (2003) The low-spin heme of cytochrome c oxidase as the driving element of the proton-pumping process. *Proc. Natl. Acad. Sci. U.S.A. 100*, 15304–15309.
16. Behr, J., Hellwig, P., Mantele, W., and Michel, H. (1998) Redox dependent changes at the heme propionates in cytochrome c oxidase from *Paracoccus denitrificans*: direct evidence from FTIR difference spectroscopy in combination with heme propionate 13C labeling. *Biochemistry 37*, 7400–7406.
17. Behr, J., Michel, H., Mantele, W., and Hellwig, P. (2000) Functional properties of the heme propionates in cytochrome c oxidase from *Paracoccus denitrificans*. Evidence from FTIR difference spectroscopy and site-directed mutagenesis. *Biochemistry 39*, 1356–1363.
18. Faxen, K., Gilderson, G., Adelroth, P., and Brzezinski, P. (2005) A mechanistic principle for proton pumping by cytochrome c oxidase. *Nature 437*, 286–289.
19. Gennis, R. B. (2004) Coupled proton and electron transfer reactions in cytochrome oxidase. *Front. Biosci. 9*, 581–591.
20. Hellwig, P., Bohm, A., Pfitzner, U., Mantele, W., and Ludwig, B. (2008) Spectroscopic study on the communication between a heme a3 propionate, Asp399 and the binuclear center of cytochrome c oxidase from *Paracoccus denitrificans*. *Biochim. Biophys. Acta 1777*, 220–226.
21. Puustinen, A., and Wikstrom, M. (1999) Proton exit from the heme-copper oxidase of *Escherichia coli*. *Proc. Natl. Acad. Sci. U.S.A. 96*, 35–37.
22. Qian, J., Mills, D. A., Geren, L., Wang, K., Hoganson, C. W., Schmidt, B., Hiser, C., Babcock, G. T., Durham, B., Millett, F., and Ferguson-Miller, S. (2004) Role of the conserved arginine pair in proton and electron transfer in cytochrome C oxidase. *Biochemistry 43*, 5748–5756.
23. Lee, H. J., Ojemyr, L., Vakkasoglu, A., Brzezinski, P., and Gennis, R. B. (2009) Properties of Arg481 mutants of the aa3-type cytochrome c oxidase from *Rhodobacter sphaeroides* suggest that neither R481 nor the nearby D-propionate of heme a3 is likely to be the proton loading site of the proton pump. *Biochemistry 48*, 7123–7131.
24. Egawa, T., Lee, H. J., Gennis, R. B., Yeh, S. R., and Rousseau, D. L. (2009) Critical structural role of R481 in cytochrome c oxidase from Rhodobacter sphaeroides. *Biochim Biophys Acta 1787*, 1272–1275.
25. Yap, L. L., Samoilova, R. I., Gennis, R. B., and Dikanov, S. A. (2007) Characterization of mutants that change the hydrogen bonding of the semiquinone radical at the QH site of the cytochrome bo3 from *Escherichia coli*. *J. Biol. Chem. 282*, 8777–8785.
26. Carrell, C. J., Ma, J. K., Antholine, W. E., Hosler, J. P., Mathews, F. S., and Davidson, V. L. (2007) Generation of novel copper sites by mutation of the axial ligand of amicyanin. Atomic resolution structures and spectroscopic properties. *Biochemistry 46*, 1900–1912.
27. Rumbley, J. N., Furlong Nickels, E., and Gennis, R. B. (1997) One-step purification of histidine-tagged cytochrome bo3 from *Escherichia coli* and demonstration that associated quinone is not required for the structural integrity of the oxidase. *Biochim. Biophys. Acta 1340*, 131–142.
28. Egawa, T., and Yeh, S. R. (2005) Structural and functional properties of hemoglobins from unicellular organisms as revealed by resonance Raman spectroscopy. *J. Inorg. Biochem. 99*, 72–96.
29. Uno, T., Mogi, T., Tsubaki, M., Nishimura, Y., and Anraku, Y. (1994) Resonance Raman and Fourier transform infrared studies on the subunit I histidine mutants of the cytochrome bo complex in *Escherichia coli*. Molecular structure of redox metal centers. *J. Biol. Chem. 269*, 11912–11920.
30. Uno, T., Nishimura, Y., Tsuboi, M., Kita, K., and Anraku, Y. (1985) Resonance Raman study of cytochrome b562-o complex, a terminal oxidase of *Escherichia coli* in its ferric, ferrous, and CO-ligated states. *J. Biol. Chem. 260*, 6755–6760.
31. Kitagawa, T., and Ozaki, Y. (1987) Infrared and Raman Spectra of Metalloporphyrins, in Metal Complexes with Tetrapyrrole Ligands I , pp 71−114, Springer, New York.
32. Spiro, T. G. (1985) Resonance Raman spectroscopy as a probe of heme protein structure and dynamics. *Adv. Protein Chem. 37*, 111–159.
33. Cheesman, M. R., Watmough, N. J., Gennis, R. B., Greenwood, C., and Thomson, A. J. (1994) Magnetic-circular-dichroism studies of *Escherichia coli* cytochrome bo. Identification of high-spin ferric, low-spin ferric and ferryl [Fe(IV)] forms of heme o. *Eur. J. Biochem. 219*, 595–602.
34. Watmough, N. J., Cheesman, M. R., Butler, C. S., Little, R. H., Greenwood, C., and Thomson, A. J. (1998) The dinuclear center of cytochrome bo3 from *Escherichia coli*. *J. Bioenerg. Biomembr. 30*, 55–62.
35. Hu, S., Smith, K. M., and Spiro, T. G. (1996) Assignment of protoheme resonance Raman spectrum by heme labeling in myoglobin. *J. Am. Chem. Soc. 118*, 12638–12646.
36. Spiro, T. G., and Wasbotten, I. H. (2005) CO as a vibrational probe of heme protein active sites. *J. Inorg. Biochem. 99*, 34–44.
37. Wang, J., Ching, Y. C., Rousseau, D. L., Hill, J. J., Rumbley, J., and Gennis, R. B. (1993) Similar carbon monoxide binding sites in bacterial cytochrome bo and mammalian cytochrome c oxidase. *J. Am. Chem. Soc. 115*, 3390–3391.
38. Hirota, S., Ogura, T., Shinzawa-Itoh, K., Yoshikawa, S., Nagai, M., and Kitagawa, T. (1994) Vibrational assignments of the FeCO unit of CO-bound heme proteins revisited: Observation of a new CO-isotope-sensitive Raman band assignable to the FeCO bending fundamental. *J. Phys. Chem. 98*, 6652–6660.
39. Rajani, C., and Kincaid, J. R. (1998) Resonance Raman studies of hemoglobin with selectively deuterated hemes. A new perspective on the controversial assignment of the Fe−CO bending mode. *J. Am. Chem. Soc. 120*, 7278–7285.
40. Guallar, V., and Olsen, B. (2006) The role of the heme propionates in heme biochemistry. *J. Inorg. Biochem. 100*, 755–760.
41. Lim, A. R., Sishta, B. P., and Mauk, A. G. (2006) Contribution of the heme propionate groups to the electron transfer and electrostatic properties of myoglobin. *J. Inorg. Biochem. 100*, 2017–2023.
42. Qin, L., Hiser, C., Mulichak, A., Garavito, R. M., and Ferguson-Miller, S. (2006) Identification of conserved lipid/detergent-binding sites in a high-resolution structure of the membrane protein cytochrome c oxidase. *Proc. Natl. Acad. Sci. U.S.A. 103*, 16117–16122.
43. Durr, K. L., Koepke, J., Hellwig, P., Muller, H., Angerer, H., Peng, G., Olkhova, E., Richter, O. M., Ludwig, B., and Michel, H. (2008) A D-pathway mutation decouples the *Paracoccus denitrificans* cytochrome c oxidase by altering the side-chain orientation of a distant conserved glutamate. *J. Mol. Biol. 384*, 865–877.
44. Aoyama, H., Muramoto, K., Shinzawa-Itoh, K., Hirata, K., Yamashita, E., Tsukihara, T., Ogura, T., and Yoshikawa, S. (2009) A peroxide bridge between Fe and Cu ions in the O2 reduction site of fully oxidized cytochrome c oxidase could suppress the proton pump. *Proc. Natl. Acad. Sci. U.S.A. 106*, 2165–2169.
45. Das, T. K., Tomson, F. L., Gennis, R. B., Gordon, M., and Rousseau, D. L. (2001) pH-dependent structural changes at the heme-copper binuclear center of cytochrome c oxidase. *Biophys. J. 80*, 2039–2045.
46. Wang, J., Takahashi, S., Hosler, J. P., Mitchell, D. M., Ferguson-Miller, S., Gennis, R. B., and Rousseau, D. L. (1995) Two conformations of the catalytic site in the aa3-type cytochrome c oxidase from *Rhodobacter sphaeroides*. *Biochemistry 34*, 9819–9825.
47. Alben, J. O., Moh, P. P., Fiamingo, F. G., and Altschuld, R. A. (1981) Cytochrome oxidase (a3) heme and copper observed by low-temperature Fourier transform infrared spectroscopy of the CO complex. *Proc. Natl. Acad. Sci. U.S.A. 78*, 234–237.
48. Fiamingo, F. G., Altschuld, R. A., and Alben, J. O. (1986) Alpha and beta forms of cytochrome c oxidase observed in rat heart myocytes by low temperature Fourier transform infrared spectroscopy. *J. Biol. Chem. 261*, 12976–12987.
49. Fiamingo, F. G., Altschuld, R. A., Moh, P. P., and Alben, J. O. (1982) Dynamic interactions of CO with a3Fe and CuB in cytochrome c oxidase in beef heart mitochondria studied by Fourier transform infrared spectroscopy at low temperatures. *J. Biol. Chem. 257*, 1639–1650.
50. Fiamingo, F. G., Jung, D. W., and Alben, J. O. (1990) Structural perturbation of the a3-CuB site in mitochondrial cytochrome c oxidase by alcohol solvents. *Biochemistry 29*, 4627–4633.
51. Mitchell, D. M., Muller, J. D., Gennis, R. B., and Nienhaus, G. U. (1996) FTIR study of conformational substates in the CO adduct of cytochrome c oxidase from *Rhodobacter sphaeroides*. *Biochemistry 35*, 16782–16788.
52. Mitchell, D. M., Shapleigh, J. P., Archer, A. M., Alben, J. O., and Gennis, R. B. (1996) A pH-dependent polarity change at the binuclear center of reduced cytochrome c oxidase detected by FTIR difference spectroscopy of the CO adduct. *Biochemistry 35*, 9446–9450.
53. Shapleigh, J. P., Hill, J. J., Alben, J. O., and Gennis, R. B. (1992) Spectroscopic and genetic evidence for two heme-Cu-containing oxidases in *Rhodobacter sphaeroides*. *J. Bacteriol. 174*, 2338–2343.
54. Wang, J., Gray, K. A., Daldal, F., and Rousseau, D. L. (1995) The cbb3-Type cytochrome c oxidase from *Rhodobacter capsulatus* contains a unique active site. *J. Am. Chem. Soc. 117*, 9363–9364.

55. Das, T. K., Pecoraro, C., Tomson, F. L., Gennis, R. B., and Rousseau, D. L. (1998) The post-translational modification in cytochrome c oxidase is required to establish a functional environment of the catalytic site. *Biochemistry 37*, 14471–14476.
56. Ji, H., Das, T. K., Puustinen, A., Wikström, M., Yeh, S. R., and Rousseau, D. L. (2009) Modulation of the active site conformation by site-directed mutagenesis in cytochrome *c* oxidase from *Paracoccus denitrificans* J. Inorg. Biochem. , in press.
57. Mills, D. A., Geren, L., Hiser, C., Schmidt, B., Durham, B., Millett, F., and Ferguson-Miller, S. (2005) An arginine to lysine mutation in the vicinity of the heme propionates affects the redox potentials of the hemes and associated electron and proton transfer in cytochrome c oxidase. *Biochemistry 44*, 10457–10465.
58. Sousa, F. L., Verissimo, A. F., Baptista, A. M., Soulimane, T., Teixeira, M., and Pereira, M. M. (2008) Redox properties of *Thermus thermophilus* ba3: different electron-proton coupling in oxygen reductases? *Biophys. J. 94*, 2434–2441.
59. Olsson, M. H., Sharma, P. K., and Warshel, A. (2005) Simulating redox coupled proton transfer in cytochrome c oxidase: looking for the proton bottleneck. *FEBS Lett. 579*, 2026–2034.
60. Seibold, S. A., Mills, D. A., Ferguson-Miller, S., and Cukier, R. I. (2005) Water chain formation and possible proton pumping routes in *Rhodobacter sphaeroides* cytochrome c oxidase: a molecular dynamics comparison of the wild type and R481K mutant. *Biochemistry 44*, 10475–10485.
61. Tashiro, M., and Stuchebrukhov, A. A. (2005) Thermodynamic properties of internal water molecules in the hydrophobic cavity around the catalytic center of cytochrome c oxidase. *J. Phys. Chem. B 109*, 1015–1022.
62. Wikstrom, M., Verkhovsky, M. I., and Hummer, G. (2003) Water-gated mechanism of proton translocation by cytochrome c oxidase. *Biochim. Biophys. Acta 1604*, 61–65.
63. Zheng, X., Medvedev, D. M., Swanson, J., and Stuchebrukhov, A. A. (2003) Computer simulation of water in cytochrome c oxidase. *Biochim. Biophys. Acta 1557*, 99–107.
64. Das, T. K., Gomes, C. M., Teixeira, M., and Rousseau, D. L. (1999) Redox-linked transient deprotonation at the binuclear site in the aa(3)-type quinol oxidase from *Acidianus ambivalens*: Implications for proton translocation. *Proc. Natl. Acad. Sci. U.S.A. 96*, 9591–9596.
65. Sharpe, M. A., and Ferguson-Miller, S. (2008) A chemically explicit model for the mechanism of proton pumping in heme-copper oxidases. *J. Bioenerg. Biomembr. 40*, 541–549.
66. Wikstrom, M., Bogachev, A., Finel, M., Morgan, J. E., Puustinen, A., Raitio, M., Verkhovskaya, M., and Verkhovsky, M. I. (1994) Mechanism of proton translocation by the respiratory oxidases. The histidine cycle. *Biochim. Biophys. Acta 1187*, 106–111.
67. Qin, L., Liu, J., Mills, D. A., Proshlyakov, D. A., Hiser, C., and Ferguson-Miller, S. (2009) Redox-dependent conformational changes in cytochrome C oxidase suggest a gating mechanism for proton uptake. *Biochemistry 48*, 5121–5130.
68. Popovic, D. M., Quenneville, J., and Stuchebrukhov, A. A. (2005) DFT/electrostatic calculations of pK(a) values in cytochrome c oxidase. *J. Phys. Chem. B 109*, 3616–3626.